Manuscripts, Articles, Book Chapters and Other Papers

8-2-2018

An eQTL Landscape of Kidney Tissue in Human Nephrotic Syndrome.

Christopher E. Gillies

Rosemary Putler

Rajasree Menon

Edgar Otto

Kalyn Yasutake

See next page for additional authors

Let us know how access to this publication benefits you

Recommended Citation

Creator(s)

Christopher E. Gillies, Rosemary Putler, Rajasree Menon, Edgar Otto, Kalyn Yasutake, Viji Nair, Paul Hoover, David Lieb, Shuqiang Li, Sean Eddy, Damian Fermin, Michelle T. McNulty, Nephrotic Syndrome Study Network (NEPTUNE), Nir Hacohen, Krzysztof Kiryluk, Matthias Kretzler, Xiaoquan Wen, Matthew G. Sampson, and Tarak Srivastava

ARTICLE

An eQTL Landscape of Kidney Tissue in Human Nephrotic Syndrome

Christopher E. Gillies,[1,8] Rosemary Putler,[1,8] Rajasree Menon,[2,8] Edgar Otto,[3] Kalyn Yasutake,[1] Viji Nair,[3] Paul Hoover,[4,5] David Lieb,[5] Shuqiang Li,[5] Sean Eddy,[3] Damian Fermin,[1] Michelle T. McNulty,[1] Nephrotic Syndrome Study Network (NEPTUNE), Nir Hacohen,[4,5] Krzysztof Kiryluk,[6] Matthias Kretzler,[2,3,9] Xiaoquan Wen,[7,9] and Matthew G. Sampson[1,9,10,*]

Expression quantitative trait loci (eQTL) studies illuminate the genetics of gene expression and, in disease research, can be particularly illuminating when using the tissues directly impacted by the condition. In nephrology, there is a paucity of eQTL studies of human kidney. Here, we used whole-genome sequencing (WGS) and microdissected glomerular (GLOM) and tubulointerstitial (TI) transcriptomes from 187 individuals with nephrotic syndrome (NS) to describe the eQTL landscape in these functionally distinct kidney structures. Using MatrixEQTL, we performed *cis*-eQTL analysis on GLOM (n = 136) and TI (n = 166). We used the Bayesian "Deterministic Approximation of Posteriors" (DAP) to fine-map these signals, eQTLBMA to discover GLOM- or TI-specific eQTLs, and single-cell RNA-seq data of control kidney tissue to identify the cell type specificity of significant eQTLs. We integrated eQTL data with an IgA Nephropathy (IgAN) GWAS to perform a transcriptome-wide association study (TWAS). We discovered 894 GLOM eQTLs and 1,767 TI eQTLs at FDR < 0.05. 14% and 19% of GLOM and TI eQTLs, respectively, had >1 independent signal associated with its expression. 12% and 26% of eQTLs were GLOM specific and TI specific, respectively. GLOM eQTLs were most significantly enriched in podocyte transcripts and TI eQTLs in proximal tubules. The IgAN TWAS identified significant GLOM and TI genes, primarily at the HLA region. In this study, we discovered GLOM and TI eQTLs, identified those that were tissue specific, deconvoluted them into cell-specific signals, and used them to characterize known GWAS alleles. These data are available for browsing and download via our eQTL browser, "nephQTL."

Introduction

Nephrotic syndrome (NS) is a rare disease of glomerular filtration barrier failure,[1,2] causing massive urinary excretion of protein, that can progress to chronic kidney disease (CKD) and end-stage renal disease (ESRD).[3,4] NS is a heterogeneous disease, so we use the histologic descriptions of glomeruli on kidney biopsy to diagnose individuals with "minimal change disease (MCD)" and "focal segmental glomerulosclerosis (FSGS)." Additionally, we use an individual's response to these treatments to give them a post hoc diagnosis of steroid-sensitive NS (SSNS) or steroid-resistant NS (SRNS).

Understanding how human genetic variation contributes to the development and progression of NS has been a fruitful strategy in gaining a more precise understanding of the molecular underpinnings of NS.[5] More than 50 genes have been discovered that harbor rare variants sufficient to cause SRNS ("Mendelian" NS).[6] Through genome-wide association studies (GWASs) and exome-chip studies,[7–10] common genetic variants have been discovered that contribute to the pathogenesis of FSGS, pediatric SSNS, and membranous nephropathy (MN). Rare variant association studies in FSGS have implicated a small set of genes harboring an increased burden of rare, deleterious variants.[8] We are challenged to discover additional forms of NS-associated genetic variation to gain biological and clinical insights.

Expression quantitative trait loci (eQTL) studies, which use mRNA expression as a proximal (and continuous) cellular endophenotype, have increased power for the discovery of statistically significant genetic effects as compared to GWASs and provides inherent biological meaning in the associations between a regulatory variant and its associated gene.[11–14] The GTEx project has generated eQTL data which is publicly available and has been used extensively to help interpret GWAS signals emerging from other complex traits.[15] Meaningful eQTL discoveries using the affected tissues in other human diseases suggest their potential for NS genomic discovery as well. This is appealing given that we often obtain kidney tissue via biopsy from affected individuals.

With regards to kidney eQTLs, the final release of GTEx will have only 73 kidney cortex samples. There is also an

absence of any other major public kidney eQTL datasets. This represents a significant barrier for genomic discovery in nephrology.

The most comprehensive kidney eQTL study thus far discovered them using unaffected portions of 96 nephrectomy samples from The Cancer Genome Atlas.[16] The investigators integrated these eQTLs with risk loci for CKD to establish links between these risk alleles and molecular mechansims.[16] A limitation of this study was that bulk renal cortex was used for association, which is known to be 80% proximal tubule cells. The preponderance of this cell type may obscure eQTL signals emerging from the structurally and cellularly heterogeneous kidney. This study also exclusively used healthy tissue, which prevents an opportunity to potentially discover disease-context-specific eQTL effects.

Microdissecting bulk renal cortex tissue into its two main functional structures, the glomerulus (GLOM) and tubulointerstitium (TI), allows increased specificity for kidney transcriptomics studies. For instance, targeted GLOM and TI eQTL studies have led to discoveries of the transcriptomic impact of diabetic kidney disease GWAS alleles in individuals with diabetic nephropathy.[17–19] In an NS GLOM eQTL study of apolipoprotein L1 (*APOL1*), ubiquitin D (*UBD*) was significantly upregulated in individuals with a high-risk (HR) *APOL1* genotype.[20] These findings were subsequently followed up in an admixture mapping study that identified enriched African ancestry at the *UBD* locus in people with a HR genotype and FSGS versus no FSGS and protective effects of *UBD* expression on the viability of cells overexpressing *APOL1* risk variants,[21] providing additional support for *UBD*'s involvement in *APOL1*-attributed NS.

The success of previous tissue-specific eQTL studies in affected populations motivated us to use this strategy for NS genomic discovery. Here, we report the results of a genome-wide GLOM and TI *cis*-eQTL study from 187 biopsied NS participants enrolled in the Nephrotic Syndrome Study Network (NEPTUNE).[22] In addition to this report, we have created "nephQTL," a publicly available eQTL browser to share these data with the wider community (Web Resources).

Material and Methods

Data Sources and Participant Inclusion
The Nephrotic Syndrome Study Network (NEPTUNE) is a prospective, longitudinal cohort recruiting participants with substantial proteinuria at the time of first kidney biopsy for clinical suspicion of minimal change disease (MCD), focal segmental glomerulosclerosis (FSGS), or membanous nephropathy (MN).[22] Phenotypic data, urine, and blood samples are collected at baseline and over time. DNA is collected for a variety of genotyping studies, and a research renal biopsy core is collected for transcriptomic analysis.[20,22–24] All procedures were done in accordance with the ethical standards of the IRBs overseeing the NEPTUNE study, and proper informed consent was obtained from each participant.

Whole-Genome Sequencing
We used Illumina Hi-Seq to perform low-depth WGS on 322 NEPTUNE participants, allowing us to take advantage of shared haplotypes and make accurate genotype calls.[25] We used GotCloud[26] as our standard pipeline for alignment and variant calling (including insertion-deletions [indels]). A subset of participants also underwent Illumina Exome Chip SNP genotyping. Using Exome chip genotypes as our gold standard, we calculated their concordance with non-monomorphic sites on WGS at 77,769 shared sites. Among heterozygous sites present in both the exome chip and WGS with minor allele frequency (MAF) > 0.05 and MAF between 0.03 and 0.05, there was 98.7% and 97.8% concordance, respectively. Site-level genotype data from WGS and the Exome Chip, summarized across this cohort, are available at our NephVS browser (Web Resources).

Gene Expression
Gene expression data from microdissected GLOM and TI were generated using Affymetrix 2.1 ST chips[27] and quantified with a Custom CDF file from BrainArray for EntrezG, v.19.[28] Expression was normalized across genes using robust multi-array average (RMA).[29] PEER factors were computed as previously described.[30]

Participant Inclusion
There were 187 NEPTUNE participants eligible for this study because they had WGS data, transcriptomic data for at least GLOM or TI, and clinical and demographic information. There were 136 and 166 available for GLOM and TI eQTL discovery, respectively. Of these, 115 participants were part of both the GLOM and TI eQTL analyses (Figure S1).

eQTL Analysis
We used MatrixEQTL[31] for the initial step in the eQTL study. We focused solely on *cis*-eQTLs because we lacked substantial power for *trans* studies. Eligible variants were those with a MAF > 0.03 in our cohort and within 500 kb of qualifying genes' transcription start or end sites (and within the gene itself). We adjusted for age, sex, principal components of genetic ancestry, and PEER factors. Principal components of genetic ancestry were calculated using EPACTS (Web Resources) on LD-pruned WGS data across all 187 individuals from whom we had expression information (Figure S2). We adjusted for the first four PCs based on visual inspection of the eigenvalue plot (Figure S3). PEER factors were created utilizing the PEER framework as previously described,[30,32] adjusting for age, sex, and microarray batch. We adjusted for 31 PEER factors in GLOM and 25 in TI, the number which, at an empirical p value threshold ($p < 1 \times 10^{-4}$), maximized the number of eQTLs discovered on chromosome 21 for that tissue. We examined the correlation of our MatrixEQTL results with and without the inclusion of a metric of NS severity, choosing baseline estimated glomerular filtration rate (eGFR). To control the FDR at gene level from the MatrixEQTL output, we used TORUS, a computationally efficient method that uses an EM (expectation maximization) algorithm to compute the prior enrichment parameters for variants.[33] The enrichment parameters computed from this procedure define a prior distribution per gene (Figure S4). The estimated priors from the GLOM and TI data can be summarized across all genes in relation to distance from the transcription start site (TSS).

Fine Mapping with DAP
We utilized the estimated priors from TORUS, accounting for variant distances to the TSS of the target genes, to perform variant

fine-mapping of eQTLs for each gene, using the Deterministic Approximation of Posteriors (DAP) algorithm.[34] Rather than solely calling eGenes (genes with significant eQTLs), DAP identifies independent eQTLs contributing significantly to changes in expression and assigns a posterior inclusion probability (PIP) to them. DAP incorporates functional genomic annotations and accounts for patterns of linkage disequilibrium (LD) among single-nucleotide polymorphisms (SNPs). Compared to calling eGenes, implicating independent eQTLs using DAP requires higher statistical stringency.

Independent association signals were either single SNPs or indels (or groups of them in LD [$r^2 > 0.25$]). The significance of each signal was characterized by local FDR. Those with local FDR < 0.05 were considered significant association signals in which we could predict the driving variants. Due to high LD and similar effect, the exact variant that drives the association signal was not always easily determined. DAP provides within-signal posterior inclusion probabilities (PIP) for each variant to help identify the most likely driver. The member SNPs for each signal group naturally form a 95% Bayesian credible set.

Tissue-Specific Mapping with eQTLBMA

To assess the extent of tissue specificity, we used eQTLBMA (eQTL by Bayesian Model Averaging) to estimate the proportion of eQTLs shared across GLOM and TI,[35] using summary statistics generated by MatrixEQTL. Partial overlapping of samples is explicitly modeled in eQTLBMA. In comparing between GLOM and TI, genes were filtered prior to running eQTLBMA to make sure that they were expressed in both tissues. This filtering process ensured that the effect sizes for each SNP/transcript pair were reliably measured in both compartments. This framework also has the benefit of maximizing power over tissue-by-tissue analysis by jointly analyzing the tissues, allowing for differences in eQTLs by tissue, and improving power for detection of shared eQTLs.

Gene Set Enrichment Analysis

To better understand the biologic context of the gene sets emerging from our DAP and eQTLBMA analyses, we used the Genomatix Software Suite (Genomatix) and Ingenuity Pathway Analysis (IPA; QIAGEN)[36] for functional annotation. In the IPA analysis, a complex network was constructed among the pathways that shared three or more genes to highlight "clusters" and pathways that crosstalk between the clusters.

Generation of Single-Cell RNA-Seq Data

We combined and analyzed three single-cell RNA-seq (scRNA-seq) datasets generated from healthy portions of tumor-nephrectomy samples specifically harvested for single-cell analysis using 10× Genomics methodology. Single-cell dissociations were done as reported.[37] Individual cells were labeled with barcodes, and transcripts within each cell were tagged with distinct UMIs (unique molecular identifiers) in order to determine absolute transcript abundance. The library quality was assessed with "high sensitivity cDNA arrays" on an Agilent Bioanalyzer (Thermo Fischer) platform. Sequencing was done on Illumina HiSeq2500 with 2 × 75 paired-end kits using the following read lengths: 26 bp Read1 and 110 bp Read2.

The sequencing data were first analyzed using the Cell Ranger software (10× Genomics Inc.) in order to extract the gene expression data matrix. Each element of the matrix is the number of UMIs associated with a gene and a barcoded cell. Next, we filtered

out cells with fewer than 500 genes per cell and with more than 25% mitochondrial read content. Further downstream analysis steps used the Seurat R package include normalization, identification of highly variable genes across the single cells, scaling based on the number of UMI and batch effect, dimensionality reduction (PCA and t-SNE), standard unsupervised clustering, and the discovery of differentially expressed cell type-specific markers. Differential gene expression to identify cell type-specific genes was performed using the non-parametric Wilcoxon rank sum test.

Cell-Type Deconvolution using Kidney Single-Cell RNA-Seq

We wanted to discover whether our significant GLOM and TI eQTLs were enriched in specific kidney cell types. We began by analyzing our adult kidney scRNA-seq data to identify genes whose expression were enriched in a particular cell type. We then computed the enrichment of GLOM and TI eGenes in these cell type-enriched gene sets using a Fisher's exact test.

Enrichment of eQTLs for Roadmap Fetal Kidney Annotations

We downloaded the full dataset of epigenomic annotations of fetal kidney from the NIH Roadmap project (Web Resources) to examine whether our eQTL variants were enriched in these annotations. As input, we used all variants within all clusters identified by DAP, and we stored the variants' PIP and their corresponding Roadmap fetal kidney annotation.

$$logit(PIP_i) \sim \ Annotation_i$$

In the above equation, "PIP_i" corresponds to the posterior inclusion probability of variant i, and $Annotation_i$ is the state of the ChromHMM model that intersects with variant i. $Annotation_i$ was coded as indicator variables for each state of the 15-state ChromHMM model, with state number 15 ("quiescent/low") as the baseline state. The result of this is a logistic regression model with 1 intercept term and 14 indicator variables, where each variant was assigned to one annotation. Significance was determined using a Wald-test of each annotation level while controlling for all other levels.

Comparison with GTEx eGenes and eQTLs

We performed three analyses to compare DAP-derived eQTLs and eGenes found in GLOM and TI with those from GTEx v.6. First, we looked up the GTEx v.6 tissue with the smallest p value for each significant SNP-eGene pair found in GLOM and TI. We then compared the difference in the –log10 p values of GLOM and TI SNP-eGene pairs with the minimum GTEx tissue. These analyses were limited to autosomes.

Second, to gain insight about eGenes unique to GLOM and TI as compared to other tissues, we used the following approach. If a significant GLOM or TI eGene was also present in the GTEx dataset and classified as an eGene in 1 of the 44 GTEx v6 tissues (per their previously described procedure[38]), we labeled the corresponding tissue an "eGene-tissue." We then summarized the distribution of the number of eGene-tissues across GTEx for all significant eGenes discovered in GLOM and TI. We also plotted GTEx liver (which has a similar number of eGenes identified as in TI) as a comparator.

Finally, to identify the magnitude of overlap between our eQTLs and those from whole blood in GTEx, we first selected GLOM and TI eQTLs with a p value < 1×10^{-5}. We chose the most significant

Table 1. Participant Characteristics for NEPTUNE Participants Included in eQTL Analyses

Characteristic	Either Expression (n = 187)	GLOM Expression (n = 136)	TI Expression (n = 166)
Age (years)	36 (17–56)	34.5 (17–55)	36 (17–56)
Pediatric	51 (27%)	39 (29%)	46 (28%)
Age of onset (years)	36 (17–56)	34.5 (17–55)	36 (17–56)
Duration of disease (months)	4 (1–18)	4 (1–17.8)	4 (1–18)
Male	131 (70%)	96 (71%)	115 (85%)
Genetic Ancestry			
AFR	54 (29%)	39 (29%)	47 (28%)
AMR	20 (11%)	13 (10%)	17 (10%)
ASN	16 (9%)	12 (9%)	15 (9%)
EUR	97 (52%)	72 (53%)	87 (52%)
Histopath			
FSGS	55 (29%)	35 (26%)	50 (30%)
MCD	37 (20%)	28 (21%)	35 (21%)
MN	41 (22%)	36 (26%)	35 (21%)
Other	54 (29%)	37 (27%)	46 (28%)
Baseline Clinical Characteristics			
RAAS blockade	130 (70%)	94 (69%)	117 (70%)
eGFR	82.5 (56.4–105.6)	83.8 (65.7–107.6)	82.4 (54.4–105.5)
UPCR	2.2 (0.8–4.2)	2 (0.6–3.9)	2.1 (0.8–3.9)
Complete remission	108 (58%)	83 (61%)	96 (58%)

Values shown are median (IQ range) or n (%). Abbreviations: AFR, African; AMR, admixed American; ASN, East Asian; EUR, European; FSGS, focal segmental glomerulosclerosis; MCD, minimal change disease; MN, membranous nephropathy; RAAS, renin-angiotensin-aldosterone system; eGFR, estimated glomerular filtration rate; UPCR, urine protein to creatinine ratio.

eSNP in this eQTL to take forward (a "SNP-eGene" pair). We then identified overlapping SNP-eGene pairs in whole blood from GTEx v6. Whole blood SNP-eGene pairs with p value $< 1 \times 10^{-3}$ were empirically defined as nominally significant and classified as overlapping with GLOM or TI eQTLs.

Comparison to Renal Cortex eGenes and eQTLs

Ko et al. have previously reported kidney cortex eQTLs[16] and published 1,886 eGenes and 124,612 SNP-eGene pairs that passed a statistical threshold of q-value < 0.05. We compared these with our GLOM and TI data in two separate analyses, recognizing that biological heterogeneity, technical and methodological differences, and availability of only a subset of cortex eQTL data must be taken into account when interpreting the data.

First, using the SNP-eGene pairs from cortex, we compared the magnitude and direction of effect of the same SNP-eGene pairs found in GLOM and TI. We then assessed the z-scores computed from cortex, GLOM, and TI via visualization and Pearson correlation. Second, we compared our significant eGene lists to those 1,886 significant cortical eGenes to identify eGenes uniquely found significant in GLOM and TI.

Transcriptome-wide Association Study with IgA Nephropathy GWASs

Previous studies have shown that risk alleles from GWASs are enriched for eQTLs,[39] and others have used eQTL data to pinpoint genes whose expression was regulated by GWAS alleles.[16] Here, we integrated our DAP-derived GLOM and TI eQTL data with summary statistics from the largest published GWAS of glomerular disease, in IgA Nephropathy[40] (IgAN), and performed a transcriptome-wide association study (TWAS) using an approach adapted from the PrediXcan and MetaXcan methods.[41,42] See Appendix A for details.

Results

Characteristics of the included participants are presented in Table 1. Approximately 30% of participants had childhood onset of disease and the median duration of disease prior to biopsy was 4 months, suggesting that we were not studying the transcriptome of participants with long-standing proteinuria. Based on genotype data, 53% and 29% of participants were of European (EUR) and African (AFR) continental ancestry, respectively. The remaining ~20% of participants were closely divided between admixed (AMR) and Asian (ASN). The histologic diagnoses were almost equally divided between MCD, FSGS, MN, and other glomerular conditions (most often IgA nephropathy).
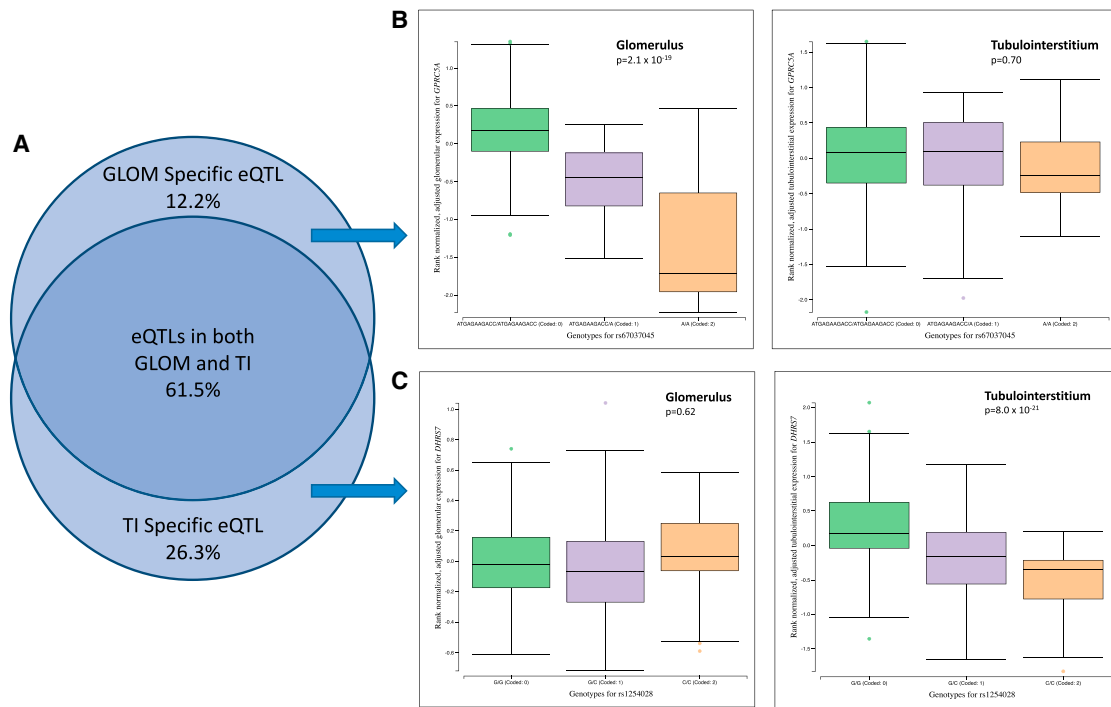
Figure 1. GLOM- and TI-Specific eQTLs from eQTLBMA
(A) Venn diagram of GLOM and TI eQTLs.
(B) Boxplot of strongest eSNPs for *GPCR5A*, among top-ranked glomerular-specific eQTL as computed by eQTLBMA. The x-axis is rs67037045 coded as 0, 1, and 2, indicating the number of non-reference alleles. The y-axis is the residuals of rank normalized *GPCR5A* expression adjusted for age, sex, batch, genetic PCs, and PEER factors.
(C) Boxplot of strongest eSNPs for *DHRS7*, among top-ranked tubulointerstitial-specific eQTL as computed by eQTLBMA. The x-axis is the rs1254028 coded as 0, 1, and 2, indicating the number of non-reference alleles. The y-axis is the residuals of rank normalized *DHRS7* expression adjusted for age, sex, batch, genetic PCs, and PEER factors.

Single SNP Analysis

Using Matrix eQTL, we analyzed 76,979,158 *cis*-pairs across 9,114,417 SNPs and expression from 22,893 genes. Based on the minimum FDR values across all eQTLs, there were 1,055 eGenes in GLOM and 3,217 eGenes in TI, at FDR < 0.05. We found a strong correlation between models that included and did not include a measure of disease severity (in this case, baseline eGFR). We used FDR of the eQTL as our metric of comparison. The overall correlation was 0.99 in both GLOM and TI. For eQTLs in which at least one model resulted in an FDR < 0.05, the correlation was 0.83 in GLOM and 0.89 in TI. Given these results, we used a model without a metric of disease severity.

Multi-SNP and Multi-tissue Analyses

The output from MatrixEQTL plus the local FDR from TORUS (Figure S4) were "fine-mapped" using DAP. Rather than solely identifying that an eQTL exists, DAP identifies eQTLs in which the specific variants or "clusters" of variants predicted to be driving the association can be confidently identified. In addition, DAP can discover eQTLs in which multiple independent SNPs or clusters of SNPs are associated with the gene's expression.

Using DAP, we discovered 894 GLOM eQTLs and 1,767 TI eQTLs at <5% FDR level (Table S1). The majority of eQTLs had one independent signal responsible for the

association. Multiple independent signals associated with expression were found in 112 GLOM eQTL (14%) and in 337 in TI (19%) (Figure S5).

To identify eQTLs that were specific to, or shared between, the GLOM and TI, we used eQTLBMA, with the MatrixEQTL data as input. We estimated 12.2% and 26.3% of eQTLs were GLOM specific and TI specific, respectively (Figure 1; Table S2). Note that this tissue specificity estimate of eQTLs is not a simple tally of individual eQTL signals. It is obtained by pooling all genes across the two tissues simultaneously, which takes the power difference in each tissue into account.

We performed gene set enrichment analysis of the DAP-derived significant GLOM and TI eQTLs using Genomatix and IPA software. Analyzing the IPA networks showed a number of immunity pathways in GLOM (Figure S6A). The TI pathways were also enriched for immunity; however, metabolic and oxidative pathways were equally as enriched (Figure S6B).

A striking aspect of the pathway enrichment analyses was the shift from inflammatory/immune-related pathways and processes in the DAP GLOM gene set to those more specific to podocyte biology with the eQTLBMA GLOM gene set. For example, eight of the top ten GO (gene ontology) biologic processes for the DAP GLOM gene set were related to antigen presentation or interferon

Table 2. Top GO Biologic Processes for GLOM-Specific eQTLs as Defined by eQTLBMA

Biological Process (GO Term)	Adjusted p Value[a]
Cell adhesion	<.001
Biological adhesion	<.001
Receptor metabolic process	<.001
Positive regulation of cytosolic calcium ion concentration	<.001
Regulation of protein kinase activity	<.001
Calcium ion transmembrane transport	<.001
Inorganic ion homeostasis	<.001
Actin cytoskeleton reorganization	.001
Cellular calcium ion homeostasis	.001
Calcium ion homeostasis	.001

[a]Adjusted p value estimated from results of 1,000 simulated null hypothesis queries (GeneRanker, Genomatix).

gamma signaling. By contrast, the top ten GO biologic processes for GLOM-specific eQTLs via eQTLBMA included actin cytoskeleton rearrangement, calcium signaling, and cell and biologic adhesion (Table 2). A StringDB network[43] created from the eQTLBMA GLOM-specific genes showed a network significantly enriched for interactions, with the two most interconnected genes being transforming growth factor beta 1 (*TGFB1*) and integrin alpha V (*ITGAV*) (Figure S7). *TGFB1* has been implicated in renal disease pathways,[44,45] including pathology of NS glomerular proteinuria.[46] *ITGAV* is a podocyte-specific essential gene candidate[47] and shows increased expression in nephritic mice.[48]

Among the most significant GLOM-specific eQTLs as computed by eQTLBMA were those of notable relevance to NS, particularly with phospholipase C gamma 2 (*PLCG2*) and vacuolar protein sorting 33b (*VPS33B*). *PLCG2* has been implicated in pediatric SSNS via genome-wide rare-variant association study.[7] *VPS33B* is a vacuolar protein and functions in vesicle-mediated protein sorting, predominantly in the late endosome/lysosome.[49] Importantly, mutations in *VPS33B* cause arthrogryposis, renal dysfunction, and cholestasis (ARC) syndrome, in which the renal phenotype includes NS.[50–52]

Cell Type Specificity of Significant GLOM and TI eQTLs

There is substantial cellular heterogeneity within the GLOM and TI which could potentially limit us from recognizing eQTLs that are cell specific or restricted to a subset of cells. We hypothesized that we could deconvolute the GLOM and TI eQTLs into specific cell types through use of independent scRNA-seq data of human kidney. Because scRNA-seq on NEPTUNE research biopsy cores is not feasible due to a lack of sufficient starting material, we integrated our eQTL data with scRNA-seq data derived from healthy portions of adult tumor nephrectomy tissue.

Single-cell transcriptome analyses of 4,734 cells identified 14 clusters of specific cell types as defined by differentially expressed cell type-specific genes (Figures 2A and S8; Table S3). The number of cells per cluster ranged from 49 in the podocyte to 1,712 within the proximal tubule. 772 and 973 genes were significantly differentially expressed in the podocyte and proximal tubule cell clusters, respectively.

As shown in Figure 2B, GLOM and TI eGenes were most significantly enriched in podocyte (OR: 2.5, $p = 8 \times 10^{-11}$) and proximal tubule cells (OR: 3.4, $p = 1 \times 10^{-43}$), respectively. We note that the GLOM eQTLs are second most enriched in proximal cells. We believe that this is a function of the microdissection process, in which we are unable to remove all proximal tubular cells from the glomeruli. Assignations of GLOM and TI eQTLs to specific cell type clusters is provided in Table S4.

We used Genomatix to annotate the 79 podocyte-specific GLOM eQTLs. The top three biologic processes (all $p < 7 \times 10^{-07}$) were "vesicle-mediated transport," "endocytosis," and "regulation of locomotion," the top molecular function was "extracellular matrix binding" ($p < 7 \times 10^{-06}$), and the top signal transduction pathway was "integrin signaling" ($p < 5 \times 10^{-05}$).

Enrichment of eQTLs for Roadmap Fetal Kidney Annotations

Both the glomerular and the tubulointerstitial eQTLs were significantly enriched in active regulatory regions in fetal kidney. In GLOM, the most significant association was annotated as "Active TSS" ($p_{GLOM} = 5.7 \times 10^{-23}$) and the second as "Enhancer" (Figure 3). The directions of effect for active regulatory regions were positively associated with higher variant PIP as compared to quiescent/low regions.

Comparison with GTEx eGenes and eQTLs

We used three different strategies to assess overlap between our DAP-derived eQTLs and those in GTEx. First, to identify GLOM and TI eQTLs whose magnitude of effect was significantly greater than in any GTEx tissue, we selected NEPTUNE eQTLs with p value $< 1 \times 10^{-5}$ (most significant per gene) and then we queried the GTEx v6 multi-tissue eQTL dataset for the same variant and gene pair (Figure S9). 53% and 66% of GLOM and TI eQTLs, respectively, had a p value < 0.001 among at least one of any GTEx tissues. 38% and 44% of GLOM and TI eQTLs, respectively, had a more significant p value in a GTEx tissue. 10% and 14% of GLOM and TI eQTLs, respectively, had a p value five orders of magnitude more significant than that found in any GTEx tissue. Given that this analysis is in part derived from a set of significant GLOM and TI eQTLs emerging from a discovery study using a 5% FDR threshold, the comparisons reported here may be interpreted with this degree of uncertainty.

Second, we observed that the majority of eGenes discovered in GLOM and TI are replicated in multiple GTEx tissues, but a substantial proportion can be confidently
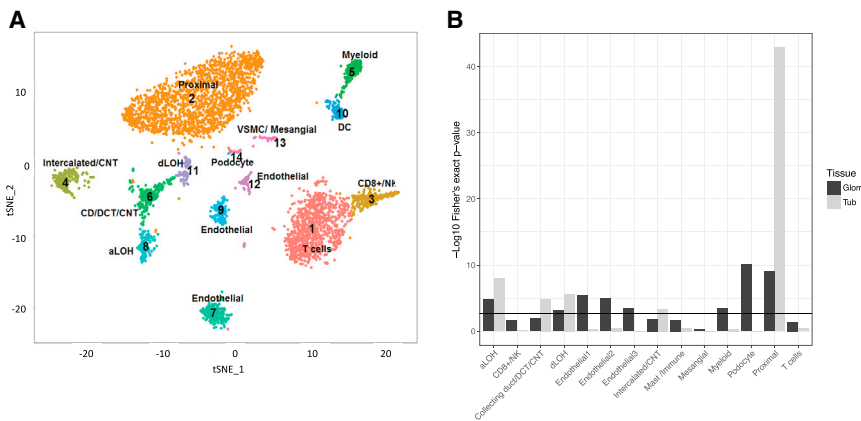
Figure 2. Results of Adult Kidney Single-Cell RNA-Seq Experiment of 4,734 Cells Resolved into 14 Clusters
(A) tSNE plot of 14 kidney cell types.
(B) Enrichment of GLOM and TI eQTLs in specific kidney cell types.
A Fisher's exact test was used to determine whether transcripts significantly enriched in one of 14 specific cell types from single-cell RNA-seq studies of adult kidney were enriched for GLOM and/or TI eQTLs. The horizontal line represents the Bonferroni corrected threshold for significance assuming 28 tests.

identified only in our data and a few other GTEx tissues (Figure S10; Table S5). Namely, 105 GLOM eGenes (12%) were not significant in any GTEx tissue; this number was 169 (9.9%) for TI eGenes. When comparing this to GTEx liver, a tissue with a similar number of eQTLs as compared to TI, we note that more liver eGenes are common to multiple other tissues.

Finally, we made a close comparison of our SNP-eGene pairs $p < 1 \times 10^{-5}$ with the same pairs in GTEx whole blood. We discovered that 26% of GLOM eQTLs with $p < 1 \times 10^{-5}$ also had a $p < 1 \times 10^{-3}$ in whole blood. In TI, 33% of eQTLs with $p < 1 \times 10^{-5}$ also had a $p < 1 \times 10^{-3}$ in whole blood.

Comparison with Renal Cortex eQTLs
Among the 124,612 significant SNP-eGene pairs identified from kidney cortex by Ko et al. and shared in their supplement,[16] 111,739 were also found in our data. For this common set of gene-SNP pairs, we compared the z-scores computed from GLOM and TI to that of cortex and found strong correlations. The Pearson correlations for GLOM-cortex and TI-cortex were 0.69 ($p < 2 \times 10^{-16}$) and 0.74 ($p < 2 \times 10^{-16}$), respectively. The scatterplots show that the vast majority of the cortex eSNPs exhibit consistent directional effect (i.e., positive or negative) in our GLOM and TI data (Figure S11). At the same time, the plots also indicate considerable effect size heterogeneity between different tissues. We also identified 655 GLOM eGenes (73%) and 1,199 TI eGenes (68%) that were not significant eGenes in cortex (Table S1, column G). These differences likely reflect a combination of tissue heterogeneity between GLOM, TI, and cortex, differences in sample sizes, and the lack of knowledge of the magnitude and direction of effect of cortex eGenes that did not pass significance thresholds.

Kidney Tissue-Based TWAS for IgAN
Using a strategy based on the MetaXcan[42] approach with minor modifications to accommodate microarray data, we predicted gene expression with a cross-validated $r^2 > 0.01$ (correlation > 0.1) in 3,294 genes from GLOM and 3,869 genes from TI. 39% of GLOM models and 42% of TI models had a cross-validated correlation > 0.2 (Table S6). Among prediction models with $r^2 > 0.01$, 73% of models in the GLOM and TI had at least ten variants selected in the prediction models. The number of variants selected in the model did not correspond to the number of independent eQTLs because the elastic net had a grouping effect where correlated variables tend to be selected or not as a group.[53] This results in linked variants being selected in the prediction model with the effect size distributed across linked variants. We discovered 13 GLOM and 12 TI eQTLs associated with IgAN with FDR < 0.1. In both tissues, decreased expression of *HLA-DRB5* had the strongest associated with IgAN (FDR$_{GLOM}$ = 8.3×10^{-6}, FDR$_{TI}$ = 3.3×10^{-9}) (Table 3; Figure S12).

Characterizing Known Kidney GWAS Alleles
We hypothesized that GLOM and TI eQTLs could be used to enhance interpretations of known GWAS alleles beyond those for NS or other glomerular diseases. For example, in one of the first GWASs of CKD, the lead SNP was rs12917707, 3.6 kb upstream of uromodulin (*UMOD*),[54] a finding that has been replicated numerous times and has led to an entire field of study regarding *UMOD* in CKD. rs12917707 is not an eQTL across 44 tissues in GTEx. By contrast, it is a significant TI eQTL in our data, with the risk allele associated with increased expression of *UMOD* (Figure S13). Our TI results are concordant with reports that the risk allele is associated with increased *UMOD* transcript expression in tumor nephrectomy tissue[55] and increased urinary protein *UMOD* expression.[56]

Discussion

Biologic insights from eQTL studies become particularly powerful when using the tissues or cells directly involved in the disease, such as adipose and muscle eQTLs for type 2 diabetes (T2D),[57] leukocytes in diverse immune-mediated diseases,[58,59] adipocytes in obesity,[60] or brain in schizophrenia.[61] Here, we used a *cis*-eQTL study design to discover genetic variants associated with steady-state mRNA levels of genes expressed in the glomeruli and
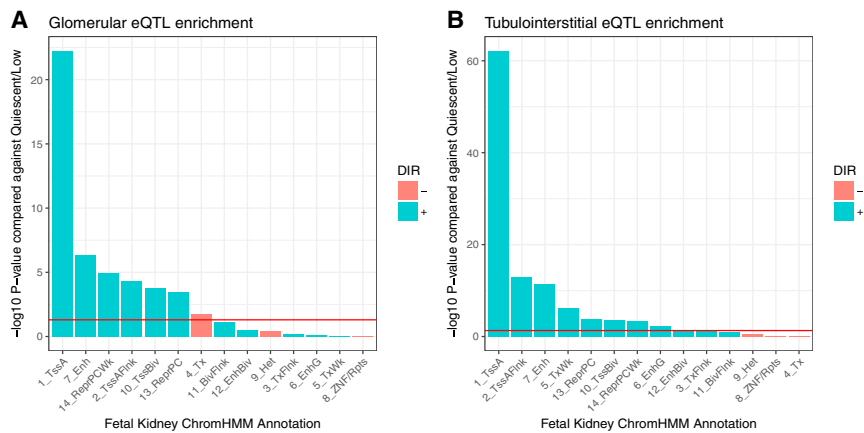
Figure 3. Glomerular and Tubulointerstitial eQTL Enrichment using Roadmap Fetal Kidney

(A) Glomerular eQTL enrichment using Roadmap fetal kidney annotation.

(B) Tubulointerstitial eQTL enrichment using Roadmap fetal kidney annotation.

We used the 15-state ChromHMM model and evaluated enrichment using logistic regression using a logit link function. We defined quiescent/low as the baseline category and coded indicator variables for the remaining 14 categories. The outcome is the variant Posterior Inclusion Probability (PIP) computed from DAP. A positive direction suggests increased enrichment of eQTLs for a particular annotation as compared to the baseline, and a negative direction of effect suggests a decreased enrichment of eQTLs compared to baseline. Abbreviations: TssA, active TSS; TssAFlnk, flanking active TSS; TxFlnk, transcription at gene 5′ & 3′; Tx, strong transcription; TxWk, weak transcription; EnhG, genic enhancers; Enh, enhancers; ZNF/Rpts, ZNF genes & repeats; Het, heterochromatin; TssBiv, bivalent/poised TSS; BivFlnk, flanking bivalent TSS/Enh; EnhBiv, bivalent enhancer; ReprPC, repressed PolyComb; ReprPCWk, weak repressed; Quies, quiescent/low.

tubulointerstitium of nephrotic syndrome individuals. Through the use of eQTLBMA and the integration of scRNA-seq data, we gained greater specificity with regards to compartment- and cell- specificity of the eQTLs we discovered. Through the integration of our results with fetal kidney tissue from Roadmap and eQTL results from GTEx, we gained additional insights into the generalizability of our results to kidney tissues without NS and human tissues other than kidney.

At a genome-wide level of significance, we discovered 894 GLOM eQTLs and 1,767 TI eQTLs in 136 and 166 eligible participants, respectively. By using multi-SNP analysis, we could fine-map these eQTLs, identifying specific SNPs with the highest probability of driving the signal, and also discovering a subset of GLOM and TI eQTL whose association is most likely to be driven by multiple, independent loci. Moving forward, narrowing the sets of implicated SNPs to identify the one that is causal, and understanding the genome biology underlying its impact on regulation will be important as we seek to discover targets and mechanism upon which we can intervene therapeutically. Given the tissue- and cell-specific nature of genomic regulatory elements, the publication and sharing of epigenetic data derived from kidney and GLOM and TI cells will be vital.

Despite biologic and technical heterogeneity between this study and that which discovered eQTLs from the renal cortex of individuals without NS, we found a strong correlation in the direction of effect and their magnitude, albeit with substantial differences in effect sizes. While the majority of GLOM and TI eGenes were not reported as significant in the cortex, we posit that these differences are driven in part by cortex eGenes that displayed the same behavior but were not significant and thus unreported. As our field begins to generate kidney-derived eQTL datasets, it should become increasingly possible to use established joint and meta-analytic methods that explicitly consider heterogeneity to compare eQTLs between studies.[62] A rigorous approach such as this could help to identify eQTLs that are compartment specific (or cell specific) as well as those that differ in disease versus healthy tissue. Making complete eQTL data available from future studies could facilitate this type of joint or meta-analysis.

When functionally annotating the DAP-significant GLOM and TI eQTLs, we observed an enrichment of immunity functions and pathways in both tissues, a not unexpected result given the known role of these pathways in NS. The cellular origins of these eQTLs are unclear, as podocytes can express these genes[63] and there are both resident immune cells[64] and circulating immune cells in the kidney. Future studies that compare eQTLs in circulating immune cells to those in the kidneys from the same individual may inform us of the contribution of each in individuals with NS. If we can ultimately link these eQTLs to clinical phenotypes, this may provide an opportunity to target the mechanism or the gene's expression level for therapeutics.

The use of eQTLBMA, integration of scRNA-seq data, and comparison to fetal kidney tissue annotations and GTEx multi-tissue eQTL provided additional insights into the inherent discoveries in this study as well as their broader applicability. The GLOM- and TI-specific eQTLs identified by eQTLBMA were enriched for processes related to the normal physiology of these compartments rather than the immune-related functions shared across tissues. Using the scRNA-seq data, we found that GLOM eQTLs were most enriched in podocytes, TI eQTLs were most enriched in the proximal tubule, and the majority of eQTLs could be assigned to a cell type. In analyzing our eQTLs in the context of fetal kidney annotations, we discovered that GLOM and TI eQTLs from NS kidney were significantly enriched within active regulatory regions annotated from fetal kidney, most strongly at active transcription start sites and enhancers. Finally, in comparing our eQTLs with those found in GTEx, we found, as expected, substantial overlap of the eQTLs between datasets. However, there were also noticeable differences, with a set of 10% and 14% of eQTLs

Table 3. Top GLOM and TI Genes Associated with IgA Nephropathy Case Status via Transcriptome-wide Association Study

Gene	FDR[a]	Direction of Expression[b]
Glomerulus		
HLA-DRB5	8.29E−06	↓
RNF5	2.24E−05	↓
HLA-DPB1	2.24E−05	↑
HLA-DQA1	3.57E−05	↑
HLA-DPA1	4.82E−04	↑
HLA-DQA2	6.95E−04	↑
HLA-DQB1	1.12E−02	↓
HLA-DQB2	4.11E−02	↓
BTN3A2	5.06E−02	↑
ZKSCAN8	5.06E−02	↓
HLA-DRB1	5.10E−02	↓
CRYBA2	7.72E−02	↑
C2orf74	7.72E−02	↓
Tubulointerstitium		
HLA-DRB5	3.29E−09	↓
HLA-DQB2	2.57E−05	↓
HLA-DQB1	1.21E−04	↓
HLA-DRB1	6.60E−04	↓
HLA-DPB1	1.19E−03	↑
ATF6B	3.01E−03	↑
HLA-DPA1	3.59E−03	↑
VWA7	1.85E−02	↓
SERPINA4	8.31E−02	↓
LAMB4	8.77E−02	↑
HIST1H4L	9.17E−02	↑
C2orf74	9.17E−02	↓

[a]FDR < 0.1
[b]Associated with IgAN cases

seemingly specific to GLOM or TI, respectively. The degree to which this heterogeneity is attributed to differences in technologies or sample size is unclear. Nevertheless, this provides an eQTL set that can be further examined for support of biologic differences driving this heterogeneity. Together, these findings should provide confidence that the data and discoveries emerging from this study may be useful beyond NS discovery.

Through a TWAS of IgAN and a single SNP lookup of the lead SNP at the CKD-associated *UMOD* locus, we demonstrated the utility of these eQTL data to gain further insights from existing GWASs of kidney disease. We focused on IgAN because, among glomerular disorders, it has the largest GWAS readily available. The ancestral composition of NEPTUNE participants (63% European or East Asian)

differed from that of IgAN GWAS (exclusively Europeans and East Asians). Previous work has shown that most eQTL effect sizes are consistent across populations,[62] and this is the assumption we made in this TWAS. Substantial heterogeneity across ancestries in this particular analysis would diminish power. However, this would not increase type 1 error.

In this TWAS, we identified a limited number of genes in which change in genetically predicted expression was associated with IgAN status. The most significant TWAS findings for IgAN that were detected independently in both tissue compartments involved decreased mRNA expression of *HLA-DRB5* ($p = 8.29 \times 10^{-6}$ in GLOM and $p = 3.29 \times 10^{-9}$ in TI compartments) with concurrent increased expression of *HLA-DPB1* ($p = 2.24 \times 10^{-5}$ in GLOM and $p = 1.19 \times 10^{-3}$ in TI compartments) and *HLA-DPA1* ($p = 4.82 \times 10^{-4}$ in GLOM and $p = 3.59 \times 10^{-3}$ in TI compartments). These genes reside under the strongest GWAS association peak for IgAN on chromosome 6p21,[40,65] but presently very little is known about the specific role of these genes in the disease pathogenesis. *HLA-DPA1* and *-DPB1* are expressed in antigen-presenting cells and encode alpha and beta chains of *HLA-DP* molecule, a membrane-anchored heterodimer responsible for presenting peptides derived from extracellular proteins. *HLA-DRB5* represents a paralog of *HLA-DRB1*, one of the most polymorphic class II molecules. The expression of *DRB5* is linked with allelic variants of *DRB1*; therefore, it is possible that this association marks the presence of specific IgAN risk alleles of the *HLA-DRB1* gene. Because these genes have not yet been experimentally tested in IgAN, further functional studies will be required to explore potential causality of these associations. Similarly, not much is presently known about the role of the other top TWAS genes (Table 3) in IgAN.

We appreciate that the causal cells for IgAN may also reside outside the kidney or that multiple hits across cell types are needed for disease pathogenesis. Future studies that perform TWASs for IgAN in other cell types and tissues will help us to clarify this issue, perhaps identifying causal genes that act in a tissue-specific manner, as has been done for other conditions.[13,60] Independent of discovering causal, tissue-specific genes, another potentially fruitful strategy could be to study the set of intrarenal genes (and their resultant networks) jointly implicated via TWASs.

We also recognize that the detected associations based on cases with NS can be quite different from the associations derived from normal kidney tissue. We view this as a potential strength of our eQTL mapping approach, since some genetic effects may be detectable only in the context of disease. At the same time, we recognize that using disease context-specific eQTLs can create an ascertainment bias in TWASs.[66] As larger GWAS datasets for other primary glomerular disorders, such as FSGS, MN, or MCD, become available, the TWAS approach should become even more relevant.

In interpreting this study overall and trying to place it in the context of similarly designed eQTL studies, there are a couple of unique characteristics to explicitly point out. First, the inclusion criteria for participants enrolled in NEPTUNE was a need for a kidney biopsy for suspicion of primary NS. There was no limitation to self-reported race, specific histologic diagnoses, eGFR, or response to immunosuppression. As such, this study should be interpreted in this light; namely that we are identifying eQTLs that are observed in the kidneys of individuals of diverse races with proteinuric glomerular filtration barrier failure.

Second, the recruitment of participants of diverse ancestries created a risk of population stratification confounding the results of this study. By following community standards, we worked to mitigate this risk through the inclusion of four PCs of genetic ancestry in the matrix eQTL model. In addition, the inclusion of PEER factors in the model should also help to account for gene expression variation attributable to population differences. Nonetheless, the transethnic design of this study should be taken into account when interpreting results. Our understanding of the potential impact of population stratification will be aided by future kidney eQTL studies from diverse ancestral populations.

With regards to heterogeneity in the causes of proteinuric kidney disease in this cohort, we found computational and experimental strategies that can be applied to GLOM and TI eQTL data to derive insights that are broadly relevant to underlying biology of these structures and specific to particular cell types. Future GLOM and TI eQTL studies in normal kidneys and those with a specific histologic or molecular diagnosis (and of similar sample sizes) would complement this study with insights about similarities and differences in the genetics of gene expression as a function of disease state.

In our opinion, sharing these eQTL and single-cell data in an easily accessible manner is just as important as any of the specific discoveries that we report here. To this end, we have added a stand-alone eQTL browser "nephQTL," to our existing NephVS software. nephQTL has a searchable browser of the summary-level MatrixEQTL and DAP output for GLOM and TI, with both summary statistics and visualizations of the eQTLs. The full MatrixEQTL output is also available for download and secondary use. For the single-cell RNA-seq data, we have also uploaded to our file sharing folder a single data matrix files with the read counts from all three tumor nephrectomy databases (see Web Resources for link). Our hope is that unrestricted access to this unique data will be useful to the wider community, catalyzing and accelerating discoveries that will ultimately lead to improved health for individuals with NS and beyond.

Appendix A: Transcriptome-wide Association Study

Using the same genotype and expression data from the eQTL analysis, we first adjusted each gene's expression by age, sex, 4 genetic PCs, and 31 PEER factors in TI and 25 in GLOM. Using the residuals for each gene, we used the R package "glmnet" to fit a regression equation penalized using an elastic net with $\alpha = 0.5$, which is a mixture of an L1 and L2 penalty. For each gene we allowed non-ambiguous biallelic variants within 500 kb of the start and end positions of each gene that were also present in the IgAN GWAS and eQTL dataset (MAF > 0.03 in the eQTL dataset). To select an appropriate hyperparameter, we used 30-fold cross-validation and selected the parameter that maximized the prediction R^2 of the validation set. We selected genes with a cross-validated prediction $R^2 > 0.01$.

Using a reference panel comprising East Asian and European samples from the 1000 Genomes data (n = 1,007 samples), for each gene g, we computed the variance of SNP 1 ($\acute{o}_l^2$) and variance of predicted expression $\acute{o}_g^2$. The variance $\acute{o}_g^2$ was defined in the MetaXcan paper as:

$$\acute{o}_g^2 = w_g' \tilde{A} w_g,$$

where w_g' is a vector of weights for gene g and $\tilde{A}$ is a covariance matrix of the SNPs included for gene g computed across the samples selected above.

Finally, we computed the Z_g statistic for gene g as:

$$Z_g \approx \sum_{l \in Model_g} w_{lg} \frac{\acute{o}_l}{\acute{o}_g} \frac{\beta_l}{se(\beta_l)}$$

where $Model_g$ is the set of SNPs for gene g, w_{lg} is the weight learned for gene g and SNP l from the elastic net, β_l is the effect size from the GWAS result for SNP l, and $se(\beta_l$ is the standard error for the effect size. We performed gene-level association using only the genes for which we could predict expression with a cross-validated $r^2 > 0.01$.

Supplemental Data

Supplemental Data include 13 figures, consortium information, and 6 tables and can be found with this article online at https://doi.org/10.1016/j.ajhg.2018.07.004.

Consortia

Members of the Nephrotic Syndrome Study Network (NEPTUNE) are as follows: John Sedor, Katherine Dell, Marleen Schachere, Kevin Lemley, Lauren Whitted, Tarak Srivastava, Connie Haney, Christine Sethna, Kalliopi Grammatikopoulos, Gerald Appel, Michael Toledo, Laurence Greenbaum, Chia-shi Wang, Brian Lee, Sharon Adler, Cynthia Nast, Janine LaPage, Ambarish Athavale, Alicia Neu, Sara Boynton, Fernando Fervenza, Marie Hogan, John C. Lieske, Vladimir Chernitskiy, Frederick Kaskel, Neelja Kumar, Patricia Flynn, Jeffrey Kopp, Eveleyn Castro-Rubio, Jodi Blake, Howard Trachtman, Olga Zhdanova, Frank Modersitzki, Suzanne Vento, Richard Lafayette, Kshama Mehta, Crystal Gadegbeku, Duncan Johnstone, Daniel Cattran, Michelle Hladunewich, Heather Reich, Paul Ling, Martin Romano, Alessia Fornoni, Laura Barisoni, Carlos Bidot, Matthias Kretzler, Debbie Gipson, Amanda Williams, Renee Pitter, Patrick Nachman, Keisha Gibson, Sandra Grubbs, Anne Froment, Lawrence Holzman, Kevin Meyers, Krishna Kallem, Fumei Cerecino, Kamal Sambandam, Elizabeth

Brown, Natalie Johnson, Ashley Jefferson, Sangeeta Hingorani, Kathleen Tuttle, Laura Curtin, S Dismuke, Ann Cooper, Barry Freedman, Jen Jar Lin, Stefanie Gray, Matthias Kretzler, Larua Barisoni, Crystal Gadegbeku, Brenda Gillespie, Debbie Gipson, Lawrence Holzman, Laura Mariani, Matthew G. Sampson, Peter Song, Johnathan Troost, Jarcy Zee, Emily Herreshoff, Colleen Kincaid, Chrysta Lienczewski, Tina Mainieri, Amanda Williams, Kevin Abbott, Cindy Roy, Tiina Urv, and John Brooks

Declaration of Interest

The authors declare no competing interests.

Web Resources

EPACTS, https://genome.sph.umich.edu/wiki/EPACTS
File sharing folder to access all MatrixEQTL output and single cell data matrix, https://umich.app.box.com/s/6jrvgmdh0ppwqvgriuvijiau0xcb4ohm
GTEx Portal, https://www.gtexportal.org/home/
NephQTL browser, http://nephQTL.org
Nephrotic syndrome variant server, http://nephvs.org
Roadmap Epigenomics, http://www.roadmapepigenomics.org/

References

1. Gipson, D.S., Selewski, D.T., Massengill, S.F., Wickman, L., Messer, K.L., Herreshoff, E., Bowers, C., Ferris, M.E., Mahan, J.D., Greenbaum, L.A., et al. (2013). Gaining the PROMIS perspective from children with nephrotic syndrome: a Midwest pediatric nephrology consortium study. Health Qual. Life Outcomes *11*, 30.

2. Rüth, E.M., Landolt, M.A., Neuhaus, T.J., and Kemper, M.J. (2004). Health-related quality of life and psychosocial adjustment in steroid-sensitive nephrotic syndrome. J. Pediatr. *145*, 778–783.

3. Kerlin, B.A., Blatt, N.B., Fuh, B., Zhao, S., Lehman, A., Blanchong, C., Mahan, J.D., and Smoyer, W.E. (2009). Epidemiology and risk factors for thromboembolic complications of childhood nephrotic syndrome: a Midwest Pediatric Nephrology Consortium (MWPNC) study. J. Pediatr. *155*, 105–110, 110.e1.

4. Hingorani, S.R., Weiss, N.S., and Watkins, S.L. (2002). Predictors of peritonitis in children with nephrotic syndrome. Pediatr. Nephrol. *17*, 678–682.

5. Sampson, M.G., and Pollak, M.R. (2015). Opportunities and challenges of genotyping patients with nephrotic syndrome in the genomic era. Semin. Nephrol. *35*, 212–221.

6. Vivante, A., and Hildebrandt, F. (2016). Exploring the genetic basis of early-onset chronic kidney disease. Nat. Rev. Nephrol. *12*, 133–146.

7. Gbadegesin, R.A., Adeyemo, A., Webb, N.J., Greenbaum, L.A., Abeyagunawardena, A., Thalgahagoda, S., Kale, A., Gipson, D., Srivastava, T., Lin, J.J., et al. (2015). HLA-DQA1 and PLCG2 are candidate risk loci for childhood-onset steroid-sensitive nephrotic syndrome. J. Am. Soc. Nephrol. *26*, 1701–1710.

8. Yu, H., Artomov, M., Brahler, S., Stander, M.C., Shamsan, G., Sampson, M.G., White, J.M., Kretzler, M., Miner, J.H., Jain, S., et al. (2016). A role for genetic susceptibility in sporadic focal segmental glomerulosclerosis. J. Clin. Invest. *126*, 1067–1078.

9. Genovese, G., Friedman, D.J., Ross, M.D., Lecordier, L., Uzureau, P., Freedman, B.I., Bowden, D.W., Langefeld, C.D., Oleksyk, T.K., Uscinski Knob, A.L., et al. (2010). Association of trypanolytic ApoL1 variants with kidney disease in African Americans. Science *329*, 841–845.

10. Okamoto, K., Tokunaga, K., Doi, K., Fujita, T., Suzuki, H., Katoh, T., Watanabe, T., Nishida, N., Mabuchi, A., Takahashi, A., et al. (2011). Common variation in GPC5 is associated with acquired nephrotic syndrome. Nat. Genet. *43*, 459–463.

11. Fairfax, B.P., Makino, S., Radhakrishnan, J., Plant, K., Leslie, S., Dilthey, A., Ellis, P., Langford, C., Vannberg, F.O., and Knight, J.C. (2012). Genetics of gene expression in primary immune cells identifies cell type-specific master regulators and roles of HLA alleles. Nat. Genet. *44*, 502–510.

12. Schadt, E.E., Molony, C., Chudin, E., Hao, K., Yang, X., Lum, P.Y., Kasarskis, A., Zhang, B., Wang, S., Suver, C., et al. (2008). Mapping the genetic architecture of gene expression in human liver. PLoS Biol. *6*, e107.

13. Musunuru, K., Strong, A., Frank-Kamenetsky, M., Lee, N.E., Ahfeldt, T., Sachs, K.V., Li, X., Li, H., Kuperwasser, N., Ruda, V.M., et al. (2010). From noncoding variant to phenotype via SORT1 at the 1p13 cholesterol locus. Nature *466*, 714–719.

14. Emilsson, V., Thorleifsson, G., Zhang, B., Leonardson, A.S., Zink, F., Zhu, J., Carlson, S., Helgason, A., Walters, G.B., Gunnarsdottir, S., et al. (2008). Genetics of gene expression and its effect on disease. Nature *452*, 423–428.

15. Battle, A., Brown, C.D., Engelhardt, B.E., Montgomery, S.B.; GTEx Consortium; Laboratory, Data Analysis &Coordinating Center (LDACC)—Analysis Working Group; Statistical Methods groups—Analysis Working Group; Enhancing GTEx (eGTEx) groups; NIH Common Fund; NIH/NCI; NIH/NHGRI; NIH/NIMH; NIH/NIDA; Biospecimen Collection Source Site—NDRI; Biospecimen Collection Source Site—RPCI; Biospecimen Core Resource—VARI; Brain Bank Repository—University of Miami Brain Endowment Bank; Leidos Biomedical—Project Management; ELSI Study; Genome Browser Data Integration &Visualization—EBI; Genome Browser Data Integration &Visualization—UCSC Genomics Institute, University of California Santa Cruz; Lead analysts; Laboratory, Data Analysis &Coordinating Center (LDACC); NIH program management; Biospecimen collection; Pathology; and eQTL manuscript working group (2017). Genetic effects on gene expression across human tissues. Nature *550*, 204–213.

16. Ko, Y.A., Yi, H., Qiu, C., Huang, S., Park, J., Ledo, N., Köttgen, A., Li, H., Rader, D.J., Pack, M.A., et al. (2017). Genetic-variation-driven gene-expression changes highlight genes with important functions for kidney disease. Am. J. Hum. Genet. *100*, 940–953.

17. Iyengar, S.K., Sedor, J.R., Freedman, B.I., Kao, W.H., Kretzler, M., Keller, B.J., Abboud, H.E., Adler, S.G., Best, L.G., Bowden, D.W., et al.; Family Investigation of Nephropathy and Diabetes (FIND) (2015). Genome-wide association and trans-ethnic meta-analysis for advanced diabetic kidney disease: Family Investigation of Nephropathy and Diabetes (FIND). PLoS Genet. *11*, e1005352.

18. Sandholm, N., Salem, R.M., McKnight, A.J., Brennan, E.P., Forsblom, C., Isakova, T., McKay, G.J., Williams, W.W., Sadlier, D.M., Mäkinen, V.P., et al.; DCCT/EDIC Research Group (2012). New susceptibility loci associated with kidney disease in type 1 diabetes. PLoS Genet. *8*, e1002921.

19. Muller, Y.L., Piaggi, P., Hanson, R.L., Kobes, S., Bhutta, S., Abdussamad, M., Leak-Johnson, T., Kretzler, M., Huang, K., Weil, E.J., et al. (2015). A cis-eQTL in PFKFB2 is associated with diabetic nephropathy, adiposity and insulin secretion in American Indians. Hum. Mol. Genet. *24*, 2985–2996.

20. Sampson, M.G., Robertson, C.C., Martini, S., Mariani, L.H., Lemley, K.V., Gillies, C.E., Otto, E.A., Kopp, J.B., Randolph, A., Vega-Warner, V., et al.; Nephrotic Syndrome Study Network (2016). Integrative genomics identifies novel associations with APOL1 risk genotypes in black NEPTUNE subjects. J. Am. Soc. Nephrol. *27*, 814–823.

21. Zhang, J.-Y., Wang, M., Tian, L., Genovese, G., Yan, P., Wilson, J.G., Thadhani, R., Mottl, A.K., Appel, G.B., Bick, A.G., et al. (2018). UBD modifies APOL1-induced kidney disease risk. Proc. Natl. Acad. Sci *115*, 3446–3451.

22. Gadegbeku, C.A., Gipson, D.S., Holzman, L.B., Ojo, A.O., Song, P.X., Barisoni, L., Sampson, M.G., Kopp, J.B., Lemley, K.V., Nelson, P.J., et al. (2013). Design of the Nephrotic Syndrome Study Network (NEPTUNE) to evaluate primary glomerular nephropathy by a multidisciplinary approach. Kidney Int. *83*, 749–756.

23. Sampson, M.G., Gillies, C.E., Robertson, C.C., Crawford, B., Vega-Warner, V., Otto, E.A., Kretzler, M., and Kang, H.M. (2016). Using population genetics to interrogate the monogenic nephrotic syndrome diagnosis in a case cohort. J. Am. Soc. Nephrol. *27*, 1970–1983.

24. Ju, W., Nair, V., Smith, S., Zhu, L., Shedden, K., Song, P.X.K., Mariani, L.H., Eichinger, F.H., Berthier, C.C., Randolph, A., et al.; ERCB, C-PROBE, NEPTUNE, and PKU-IgAN Consortium (2015). Tissue transcriptome-driven identification of epidermal growth factor as a chronic kidney disease biomarker. Sci. Transl. Med. *7*, 316ra193.

25. Li, Y., Sidore, C., Kang, H.M., Boehnke, M., and Abecasis, G.R. (2011). Low-coverage sequencing: implications for design of complex trait association studies. Genome Res. *21*, 940–951.

26. Jun, G., Wing, M.K., Abecasis, G.R., and Kang, H.M. (2015). An efficient and scalable analysis framework for variant extraction and refinement from population-scale DNA sequence data. Genome Res. *25*, 918–925.

27. Cohen, C.D., Frach, K., Schlöndorff, D., and Kretzler, M. (2002). Quantitative gene expression analysis in renal biopsies: a novel protocol for a high-throughput multicenter application. Kidney Int. *61*, 133–140.

28. Dai, M., Wang, P., Boyd, A.D., Kostov, G., Athey, B., Jones, E.G., Bunney, W.E., Myers, R.M., Speed, T.P., Akil, H., et al.

(2005). Evolving gene/transcript definitions significantly alter the interpretation of GeneChip data. Nucleic Acids Res. *33*, e175–e175.

29. Lockstone, H.E. (2011). Exon array data analysis using Affymetrix power tools and R statistical software. Brief. Bioinform. *12*, 634–644.

30. Stegle, O., Parts, L., Durbin, R., and Winn, J. (2010). A Bayesian framework to account for complex non-genetic factors in gene expression levels greatly increases power in eQTL studies. PLoS Comput. Biol. *6*, e1000770.

31. Shabalin, A.A. (2012). Matrix eQTL: ultra fast eQTL analysis via large matrix operations. Bioinformatics *28*, 1353–1358.

32. Parts, L., Stegle, O., Winn, J., and Durbin, R. (2011). Joint genetic analysis of gene expression data with inferred cellular phenotypes. PLoS Genet. *7*, e1001276.

33. Wen, X. (2016). Molecular QTL discovery incorporating genomic annotations using Bayesian false discovery rate control. Ann. Appl. Stat. *10*, 1619–1638.

34. Wen, X., Lee, Y., Luca, F., and Pique-Regi, R. (2016). Efficient integrative multi-SNP association analysis via deterministic approximation of posteriors. Am. J. Hum. Genet. *98*, 1114–1129.

35. Flutre, T., Wen, X., Pritchard, J., and Stephens, M. (2013). A statistical framework for joint eQTL analysis in multiple tissues. PLoS Genet. *9*, e1003486.

36. Krämer, A., Green, J., Pollard, J., Jr., and Tugendreich, S. (2014). Causal analysis approaches in Ingenuity Pathway Analysis. Bioinformatics *30*, 523–530.

37. Rao, D.A., Berthier, C.C., Arazi, A., Davidson, A., Liu, Y., Browne, E.P., Eisenhaure, T.M., Chicoine, A., Lieb, D.J., Smilek, D.E., et al. (2018). A protocol for single-cell transcriptomics from cryopreserved renal tissue and urine for the Accelerating Medicine Partnership (AMP) RA/SLE network. bioRxiv. 275859; doi: https://doi.org/10.1101/275859.

38. Consortium, G.T.; and GTEx Consortium (2015). Human genomics. The Genotype-Tissue Expression (GTEx) pilot analysis: multitissue gene regulation in humans. Science *348*, 648–660.

39. Nicolae, D.L., Gamazon, E., Zhang, W., Duan, S., Dolan, M.E., and Cox, N.J. (2010). Trait-associated SNPs are more likely to be eQTLs: annotation to enhance discovery from GWAS. PLoS Genet. *6*, e1000888.

40. Kiryluk, K., Li, Y., Scolari, F., Sanna-Cherchi, S., Choi, M., Verbitsky, M., Fasel, D., Lata, S., Prakash, S., Shapiro, S., et al. (2014). Discovery of new risk loci for IgA nephropathy implicates genes involved in immunity against intestinal pathogens. Nat. Genet. *46*, 1187–1196.

41. Gamazon, E.R., Wheeler, H.E., Shah, K.P., Mozaffari, S.V., Aquino-Michaels, K., Carroll, R.J., Eyler, A.E., Denny, J.C., Nicolae, D.L., Cox, N.J., Im, H.K.; and GTEx Consortium (2015). A gene-based association method for mapping traits using reference transcriptome data. Nat. Genet. *47*, 1091–1098.

42. Barbeira, A.N., Dickinson, S.P., Bonazzola, R., Zheng, J., Wheeler, H.E., Torres, J.M., Torstenson, E.S., Shah, K.P., Garcia, T., Edwards, T.L., et al.; GTEx Consortium (2018). Exploring the phenotypic consequences of tissue specific gene expression variation inferred from GWAS summary statistics. Nat. Commun. *9*, 1825.

43. Franceschini, A., Szklarczyk, D., Frankild, S., Kuhn, M., Simonovic, M., Roth, A., Lin, J., Minguez, P., Bork, P., von Mering, C., and Jensen, L.J. (2013). STRING v9.1: protein-protein interaction networks, with increased coverage and integration. Nucleic Acids Res. *41*, D808–D815.

44. Gagliardini, E., and Benigni, A. (2006). Role of anti-TGF-beta antibodies in the treatment of renal injury. Cytokine Growth Factor Rev. *17*, 89–96.

45. Böttinger, E.P., and Bitzer, M. (2002). TGF-beta signaling in renal disease. J. Am. Soc. Nephrol. *13*, 2600–2610.

46. Cevikbas, F., Schaefer, L., Uhlig, P., Robenek, H., Theilmeier, G., Echtermeyer, F., and Bruckner, P. (2008). Unilateral nephrectomy leads to up-regulation of syndecan-2- and TGF-beta-mediated glomerulosclerosis in syndecan-4 deficient male mice. Matrix Biol. *27*, 42–52.

47. Lu, Y., Ye, Y., Bao, W., Yang, Q., Wang, J., Liu, Z., and Shi, S. (2017). Genome-wide identification of genes essential for podocyte cytoskeletons based on single-cell RNA sequencing. Kidney Int. *92*, 1119–1129.

48. Toda, N., Mori, K., Kasahara, M., Ishii, A., Koga, K., Ohno, S., Mori, K.P., Kato, Y., Osaki, K., Kuwabara, T., et al. (2017). Crucial role of mesangial cell-derived connective tissue growth factor in a mouse model of anti-glomerular basement membrane glomerulonephritis. Sci. Rep. *7*, 42114.

49. Gissen, P., Johnson, C.A., Gentle, D., Hurst, L.D., Doherty, A.J., O'Kane, C.J., Kelly, D.A., and Maher, E.R. (2005). Comparative evolutionary analysis of VPS33 homologues: genetic and functional insights. Hum. Mol. Genet. *14*, 1261–1270.

50. Gissen, P., Johnson, C.A., Morgan, N.V., Stapelbroek, J.M., Forshew, T., Cooper, W.N., McKiernan, P.J., Klomp, L.W., Morris, A.A., Wraith, J.E., et al. (2004). Mutations in VPS33B, encoding a regulator of SNARE-dependent membrane fusion, cause arthrogryposis-renal dysfunction-cholestasis (ARC) syndrome. Nat. Genet. *36*, 400–404.

51. Weyand, A.C., Lombel, R.M., Pipe, S.W., and Shavit, J.A. (2016). The role of platelets and epsilon-aminocaproic acid in arthrogryposis, renal dysfunction, and cholestasis (ARC) syndrome associated hemorrhage. Pediatr. Blood Cancer *63*, 561–563.

52. Holme, A., Hurcombe, J.A., Straatman-Iwanowska, A., Inward, C.I., Gissen, P., and Coward, R.J. (2013). Glomerular involvement in the arthrogryposis, renal dysfunction and cholestasis syndrome. Clin. Kidney J. *6*, 183–188.

53. Zou, H., and Hastie, T. (2005). Regularization and variable selection via the elastic net. J. R. Stat. Soc. Series B Stat. Methodol. *67*, 301–320.

54. Köttgen, A., Glazer, N.L., Dehghan, A., Hwang, S.J., Katz, R., Li, M., Yang, Q., Gudnason, V., Launer, L.J., Harris, T.B., et al. (2009). Multiple loci associated with indices of renal function and chronic kidney disease. Nat. Genet. *41*, 712–717.

55. Trudu, M., Janas, S., Lanzani, C., Debaix, H., Schaeffer, C., Ikehata, M., Citterio, L., Demaretz, S., Trevisani, F., Ristagno, G., et al.; SKIPOGH team (2013). Common noncoding UMOD gene variants induce salt-sensitive hypertension and kidney damage by increasing uromodulin expression. Nat. Med. *19*, 1655–1660.

56. Olden, M., Corre, T., Hayward, C., Toniolo, D., Ulivi, S., Gasparini, P., Pistis, G., Hwang, S.J., Bergmann, S., Campbell, H., et al. (2014). Common variants in UMOD associate with urinary uromodulin levels: a meta-analysis. J. Am. Soc. Nephrol. *25*, 1869–1882.

57. Sajuthi, S.P., Sharma, N.K., Chou, J.W., Palmer, N.D., McWilliams, D.R., Beal, J., Comeau, M.E., Ma, L., Calles-Escandon, J., Demons, J., et al. (2016). Mapping adipose and muscle tissue expression quantitative trait loci in African Americans to identify genes for type 2 diabetes and obesity. Hum. Genet. *135*, 869–880.

58. Walsh, A.M., Whitaker, J.W., Huang, C.C., Cherkas, Y., Lamberth, S.L., Brodmerkel, C., Curran, M.E., and Dobrin, R. (2016). Integrative genomic deconvolution of rheumatoid arthritis GWAS loci into gene and cell type associations. Genome Biol. *17*, 79.

59. Peters, J.E., Lyons, P.A., Lee, J.C., Richard, A.C., Fortune, M.D., Newcombe, P.J., Richardson, S., and Smith, K.G. (2016). Insight into genotype-phenotype associations through eQTL mapping in multiple cell types in health and immune-mediated disease. PLoS Genet. *12*, e1005908.

60. Claussnitzer, M., Dankel, S.N., Kim, K.H., Quon, G., Meuleman, W., Haugen, C., Glunk, V., Sousa, I.S., Beaudry, J.L., Puviindran, V., et al. (2015). FTO obesity variant circuitry and adipocyte browning in humans. N. Engl. J. Med. *373*, 895–907.

61. Sekar, A., Bialas, A.R., de Rivera, H., Davis, A., Hammond, T.R., Kamitaki, N., Tooley, K., Presumey, J., Baum, M., Van Doren, V., et al.; Schizophrenia Working Group of the Psychiatric Genomics Consortium (2016). Schizophrenia risk from complex variation of complement component 4. Nature *530*, 177–183.

62. Wen, X., Luca, F., and Pique-Regi, R. (2015). Cross-population joint analysis of eQTLs: fine mapping and functional annotation. PLoS Genet. *11*, e1005176.

63. Goldwich, A., Burkard, M., Olke, M., Daniel, C., Amann, K., Hugo, C., Kurts, C., Steinkasserer, A., and Gessner, A. (2013). Podocytes are nonhematopoietic professional antigen-presenting cells. J. Am. Soc. Nephrol. *24*, 906–916.

64. Rogers, N.M., Ferenbach, D.A., Isenberg, J.S., Thomson, A.W., and Hughes, J. (2014). Dendritic cells and macrophages in the kidney: a spectrum of good and evil. Nat. Rev. Nephrol. *10*, 625–643.

65. Gharavi, A.G., Kiryluk, K., Choi, M., Li, Y., Hou, P., Xie, J., Sanna-Cherchi, S., Men, C.J., Julian, B.A., Wyatt, R.J., et al. (2011). Genome-wide association study identifies susceptibility loci for IgA nephropathy. Nat. Genet. *43*, 321–327.

66. Lin, D.Y., and Zeng, D. (2009). Proper analysis of secondary phenotype data in case-control association studies. Genet. Epidemiol. *33*, 256–265.